X-ray diffraction characterization of dental gold alloy-ceramic interfaces

Z. CAI*, I. WATANABE[1], J. C. MITCHELL[2], W. A. BRANTLEY[3], T. OKABE
Department of Biomaterials Science, Baylor College of Dentistry, The Texas A&M University System Health Science Center, Dallas, TX, USA
[1]Department of Fixed Prosthodontics, Nagasaki University School of Dentistry, Nagasaki, Japan
[2]Department of Geological Sciences and [3]College of Dentistry, The Ohio State University, Columbus, OH, USA
E-mail: zcai@tambcd.edu

X-ray diffraction (XRD) was employed to study dental alloy-ceramic interfaces. A Au-Pd-In alloy, which requires oxidation before porcelain firing, and a Au-Pt-Pd-In alloy, which does not require oxidation before porcelain firing, were selected in this study. Alloy specimens were centrifugally cast. Specimen surfaces were metallographically polished through 0.05 μm Al_2O_3 slurries. A thin layer (< 50 μm) of a dental opaque porcelain was fired on the alloy surfaces with and without initial oxidation. XRD was conducted at room temperature on four types of alloy specimens: polished, oxidized, porcelain fired after alloy oxidation, and porcelain fired without initial alloy oxidation. XRD was also performed on fired opaque porcelain without an alloy substrate. The detection of prominent gold solid solution peaks from alloy-ceramic specimens indicated that the incident X-ray beam reached the alloy-ceramic interface. In_2O_3 and β-Ga_2O_3 were identified on the oxidized Au-Pd-In alloy, while In_2O_3 and SnO_2 were detected on the oxidized Au-Pt-Pd-In alloy. Preferred orientation was observed for all the oxides formed on the alloys. Minimum lattice parameter changes ($< 1\%$) for the gold solid solutions were observed for both alloys before and after oxidation and porcelain firing. Leucite ($KAlSi_2O_6$), TiO_2, ZrO_2 and SnO_2 were detected on the fired opaque porcelain. For both alloys, no additional oxides were identified at the metal-ceramic interfaces beyond those present in the oxidized alloys and the opaque porcelain. Similar results were obtained from alloy-ceramic interfaces where there was no prior alloy oxidation. The results indicate the critical role of alloy surface oxides in metal-ceramic bonding and support the chemical bonding mechanism for porcelain adherence.

1. Introduction

As a major esthetic restorative method in prosthodontics [1] that provided a significant advancement in oral functional reconstruction [2], the use of metal-ceramic restorations has experienced great success since their early commercial introduction to the dental profession more than three decades ago [3, 4]. They represent a significant advancement in oral prosthetic and functional reconstruction [2], and are considered to be the strongest and the most durable ceramic restorations available today [5]. The success of metal-ceramic systems has been documented in *in vitro* [6] and long-term clinical studies [7]. The overall clinical survival rates for metal-ceramic restorations are far superior to any of the all-ceramic systems [8]. Durability and long-lasting esthetic qualities are the most outstanding benefits of metal-ceramic restorations, which combine the strength, toughness, accuracy and marginal adaptation of metals with the permanent esthetic appearance of ceramics [9, 10]. Because of these properties, it has been suggested that metal-ceramic systems will continue to be used as a main restorative method in the twenty first century [11].

The properties of metal-ceramic restorations depend critically upon the nature of the interface between the alloy and porcelain. When intimate contact is established between the metal and ceramic surfaces, there is a reduction in free energy compared to that for the two separate components [12, 13]. Although the adherence of modern dental porcelains (borosilicate feldspathic glasses with oxide filler particles [14]) to metal castings has been studied for over three decades, the exact bonding mechanism remains elusive due to the complex

*Author to whom all correspondence should be addressed.
This study was presented at the 27th Annual Meeting of American Association for Dental Research Minneapolis, MN, March, 1998.

nature of these restorative materials [15, 16]. It is generally recognized that three contributions to interfacial bonding are applicable in varying degrees: chemical bonding, mechanical interlocking, and van der Waals forces [15, 17, 18].

Based on study of the wetting of a sodium silicate glass on several pure metal substrates, Pask and Fulrath [19] proposed that chemical bonding develops when there is a balance of bond energies across the transition zone between metal and glass. It was considered that the dissolved oxide undergoes diffusion from the molten glass interface into the bulk of the liquid glass until a saturated continuous solid solution is formed. Because the chemical bonding in glass and oxide are similar in nature, a balance of chemical bonds may exist, and chemical bonds across the glass-metal phase boundary may be maintained [20]. Chemical bonding was defined as occurring when there is localized charge transport across the interface as a metal and ceramic are brought into contact over interatomic distances [13].

The chemical bonding theory is considered applicable to complex dental alloy and porcelain systems [15]. Segregation of oxidizable elements (Fe, Sn, Cu) in a gold alloy, within a few microns of the metal-ceramic interface [21, 22], suggested that an equilibrium of trace metal oxides across the interface was responsible for chemical bonding in this system. For Au-Pt-Pd alloy, the formation of base metal ions (Sn, Fe and In) and their diffusion to the oxide-air interface were considered as the rate-limiting steps for alloy oxidation [23]. Wagner *et al*. [24] showed that improved porcelain bonding to a palladium alloy surface was attributed to pre-oxidation and surface roughening of the alloy; substantially reduced bonding to alloy samples was observed when the porcelain was fired in a reducing atmosphere.

Studies on both noble and base metal alloys have shown that the alloys which form adherent oxides during porcelain firing also form strong bonds to porcelain, whereas those alloys with poorly adherent oxides form weak bonds [25, 26]. Suppression of Cr, Ni and Co ion diffusion to the metal-ceramic interface during porcelain firing through the use of a bonding agent may improve the ceramic bonding to base metal alloys; it has been proposed that the mechanism of the resulting enhanced oxide adherence arises from a reduction in the vacancy concentration at the metal-oxide interface [27].

The contribution of van der Waals forces to dental metal-ceramic bonding is considered to be relatively small. It was shown that such forces can theoretically provide sufficient bond strength when there is adequate wettability of the porcelain on the oxidized metal surface over interatomic distances [28]. Appropriate wetting of the liquid porcelain on the metal surface at high temperatures is necessary to achieve both chemical bonding and van der Waals bonding, the latter occurring without an equilibrium transition zone at the interface. It is now recognized that wetting alone is not sufficient to ensure good bonding [15].

Several studies have shown that mechanical interlocking produced by increasing the roughness of the metal surfaces improved the metal-ceramic adherence [24, 29, 30]. An increase in the surface roughness of the metal substrate may also improve its wettability by porcelain and provide increased surface area for chemical bonding [1, 31]. However, an excessively rough metal substrate surface may decrease the fracture resistance of porcelain by concentrating stress at the metal-ceramic interface and may also prevent complete wetting of the ceramic forming voids at the interface [29, 32].

Besides surface roughness, the other critical physical factor in metal-ceramic bonding is the thermal expansion/contraction behavior of the two components. The coefficients of thermal contraction (CTC) for both the metal and ceramic below the glass transition temperature (T_g) of the porcelain must be closely matched to avoid deleterious tensile stress at the interface. It is generally considered that the CTC for the ceramic should be $0.5 - 1 \times 10^{-6}/0$C less than that for the metal in order to strengthen the ceramic by retaining a slight residual compressive stress [33]. The heating and cooling rate during porcelain firing is an important factor, since the values of CTC and T_g for the porcelain change with different heating or cooling rates [34–38]. The geometry of the metal–ceramic restoration also affects the bonding by changing the stress distribution at the interface [39].

Because of the difficulty in precisely specifying the mechanisms for adhesion and the impossibility of determining a true metal-ceramic bond strength in the absence of residual stresses and interfacial stress concentrations, O'Brien [40] proposed the cohesive plateau theory as a general approach to metal-ceramic bonding. This approach depends upon no specific source of adhesion, and the emphasis is on determining the mode of metal-ceramic failure rather than an interfacial bond strength. Optimum metal-ceramic bonding is recognized as when bond failure occurred in the ceramic layer.

X-ray diffraction (XRD) is a useful surface analysis technique [41] for the study of dental alloy oxidation [42, 43] and metal-ceramic interfaces. In a study on the oxidation of dental alloys and the oxides formed at the alloy-ceramic interfaces [44, 45], XRD was employed. XRD was used to characterize the effect of oxidation at dental porcelain firing temperatures on the surface oxidation and lattice parameter changes on dental alloys [46]. In another study [47], XRD was used to characterize enamel-steel interfaces. The objective of the present study was to employ an XRD technique to characterize the high-temperature oxidation of two noble dental alloys and the alloy-ceramic interfaces.

2. Materials and methods

Two commercial gold-based dental alloys for metal-ceramic application were selected in this study. The compositions of the alloys are provided in Table I. High-temperature oxidation behavior of these two alloys has not been reported. According to the manufacturers, the Au-Pd Orion alloy requires oxidation before firing porcelain, whereas no oxidation is required for the Au-Pt-Pd Enaglaz I alloy before porcelain firing to achieve the optimum alloy-ceramic adhesion.

Alloy specimens (10 mm × 10 mm × 1 mm) were cast with a conventional multiorifice gas-oxygen torch and centrifugally cast in air into a phosphate-bonded

TABLE I Compositions (wt %) of the metal-ceramic alloys used in this study*

	Au	Pt	Pd	In	Ag	Other
Orion†	51	–	39	8	–	Ga, Re
Enaglaz I‡	74.9	14.8	6.2	2.2	0.5	Sn

*Data were provided by the manufacturers.
†Ney, Bloomfield, CT, USA.
‡Tokuriki Honten, Tokyo, Japan.

investment (Power Cast, Whip Mix, Louisville, KY, USA). Two specimens were prepared for each alloy. Following standard dental laboratory procedures, the castings were bench-cooled in air, devested and air-abraded with 50 μm Al_2O_3 particles. Specimen surfaces were subsequently metallographically polished using a series of abrasives through 0.05 μm Al_2O_3 slurries and ultrasonically cleaned in distilled water. Polished specimens were not etched before being examined by XRD.

Oxidation of the two alloys was performed in a dental furnace (Vacumat 100, Vident, Baldwin Park, CA, USA) in air as recommended by the manufacturer for the Orion alloy (Ney); each alloy was heated from 649 °C to 1038 °C at 32 °C/min with a 3 min hold period at the peak temperature. In order to ensure that the incident X-ray beam would reach the metal-ceramic interfaces, a very thin layer (< 50 μm) of an opaque dental porcelain (VMK 68, A3 212, VITA Zahnfabrik H., Bad Säckingen, Germany) was fired on the specimen surfaces following the manufacturer's instructions (heat from 650 °C to 990 °C at 32 °C/min in air). Approximately 3 mg of the opaque porcelain powder was mixed with distilled water and dispensed uniformly on the specimen surface using an ultrasonic ceramic condenser (Ceramosonic Condenser, Unitek, Monrovia, CA, USA). The thickness of the opaque porcelain fired on the substrate was determined by measuring with a micrometer having a precision of 10 μm. XRD was performed on four types of specimen surfaces for each of the two alloys: polished alloy, oxidized alloy, porcelain fired on the oxidized alloy, and porcelain fired on the alloy without initial oxidation. In order to further verify the origin of oxides on polished specimens, an additional specimen was prepared for each alloy. Two disk-shaped specimens (6 mm diameter, 3 mm thick) of opaque porcelain (VMK 68, A3 212) without a metal substrate were also fired following the manufacturer's recommendations, and polished through 600 grit SiC paper. Additional opaque porcelain powder specimens were prepared by grinding the disk-shaped specimens into fine powder using pestle and mortar.

The XRD patterns for all the specimens were obtained at room temperature, using Cu Kα radiation on two X-ray diffractometers. XRD patterns for the specimens under all of the four alloy surface conditions and the fired opaque porcelain disk specimens were obtained using an X-ray diffractometer ($\lambda = 1.5418$ Å) (Miniflex CN2005 Rigaku, Tokyo, Japan) equipped with a Ni filter, operating over a 2θ range of 25–90° at a continuous scan rate of 0.5°/min. This diffractometer is routinely calibrated using a silicon standard (640b Silicon Powder XRD Spacing, Standard Reference Material, National Institute of Standards and Technology, Gaithersburg, MD, USA). In addition, XRD patterns for the polished and porcelain-fired alloy specimens, and the fired opaque porcelain powder specimen, were also obtained on a diffractometer with a high-precision, wide-range goniometer (Philips Electronics PW 1316/90, Philips, Eindhoven, The Netherlands), an XRG 3100 X-ray generator ($\lambda = 1.5406$ Å), DMS-41 measuring system and graphite monochromator over a 2θ range from 25–85° at step intervals of 0.03° and a photon-counting time of 4 s per step.

The peaks of the XRD patterns were indexed to the ICDD (International Center for Diffraction Data, Swarthmore, PA) polycrystalline powder diffraction files. The Nelson-Riley analysis [41] was used with linear regression analysis to determine the lattice parameter of the gold solid solutions from the position of the 111, 200, 220, 311 and 222 peaks. Data from both diffractometers were used for the gold solid solution *d*-spacing calculations for the polished and porcelain-fired alloy specimens, while calculations for the oxidized specimens were based on the data from the Rigaku diffractometer.

3. Results

The XRD patterns for both the polished Orion and Enaglaz I alloys showed high-intensity face-centered cubic (fcc) gold solid solution peaks. Consistent results were obtained from the two diffractometers, with values of d-spacings for the same specimen condition agreeing within approximately 0.02 Å. The XRD powder diffraction files employed to index the oxides are listed in Table II. Compared to the polycrystalline gold powder

TABLE II X-ray powder diffraction files* for oxides identified in the present study

Oxide	Structure	ICDD Standard
In_2O_3	Cubic	6–416
β-Ga_2O_3	Monoclinic	41–1103
SnO_2 (cassiterite)	Tetragonal	21–1250
($KAlSi_2O_6$) (leucite)	Tetragonal	15–47
TiO_2 (rutile)	Tetragonal	21–1276
ZrO_2 (baddeleyite)	Monoclinic	37–1484

*International Center for Diffraction Data (ICDD), Swarthmore, PA, USA.

diffraction files (ICDD 4–784), slight preferred crystallographic orientation for the gold solid solution was observed in the two polished alloys. For polished Orion, additional low-intensity peaks were identified as β-Ga_2O_3 and In_2O_3 peaks. A low-intensity peak at $2\theta = 50.18°$ could not be matched to the two oxide diffraction card files and is considered to arise from some unidentified secondary phase in the alloy. A low-intensity peak on the Enaglaz I XRD pattern was considered to be from SnO_2 while the peak at $2\theta = 36.98°$ is attributed to an unidentified secondary phase in this alloy. Since the XRD patterns for polished specimens were initially acquired several weeks after the surface polishing, additional XRD patterns were obtained for each alloy on the third specimen immediately after the polishing. Consistent results were observed for both polished specimens for each alloy.

On the XRD patterns for the oxidized Orion specimens, prominent gold solid solution peaks were observed in addition to In_2O_3 and β-Ga_2O_3 peaks associated with the oxide layer on the alloy surface. The d-spacings for the oxide peaks matched the ICDD powder diffraction files within 0.01 Å. A peak with a d-spacing of 2.23 Å ($2\theta = 40.45°$) could not be matched to either In_2O_3 or β-Ga_2O_3 and remains unidentified. Comparisons of the peak positions on the XRD pattern with ICDD powder diffraction files for δ-Ga_2O_3(ICDD 6 − 529), γ-Ga_2O_3 (ICDD 20–426), β-$GaInO_3$ (ICDD 21–334) $GaInO_3$ (ICDD 21–333) and $(Ga,In)_2O_3$ (ICDD 14–564) suggested that these phases were not present on the surface oxide layer. When relative intensities of the peaks were compared to the polycrystalline powder diffraction files, substantial preferred orientation was observed for the oxides (In_2O_3 and β-Ga_2O_3) formed on the alloy surfaces.

Both cubic In_2O_3 and tetragonal SnO_2 were identified on oxidized Enaglaz I. Excellent matches were found between the peaks observed and the ICDD powder diffraction files, except for two In_2O_3 peaks ($d = 2.946$ Å and $d = 2.550$ Å whose d-spacings were about 0.02 Å larger than those for the powder diffraction files. Two peaks with d-spacings of 1.411 Å and 1.200 Å may correspond to overlapping peaks from the two oxides. A peak with a d-spacing of 2.596 Å ($2\theta = 34.55°$) did not match either of the two ICDD powder diffraction files and was not identified. Comparisons of the peak positions from the powder diffraction files of In_2SnO_5 (ICDD 32–458) and $In_2Sn_2O_{7-x}$ (ICDD 39–1058) with the XRD patterns suggested that these oxides were not present in the surface oxide layer. Preferred crystallographic orientation was also observed for both In_2O_3 and SnO_2 on oxidized Enaglaz I.

On the fired opaque VMK 68 porcelain disk specimens, leucite ($KAlSi_2O_6$) (ICDD 15–47), TiO_2 (ICDD 21–1276), ZrO_2 (ICDD 37–1484) and SnO_2 were detected. Consistent results were obtained from the two disk specimens. Peaks with d-spacings of 3.18 Å, 2.845 Å, 2.379 Å, and between 1.678 Å to 1.418 Å corresponded to overlapping peaks from multiple oxides. Preferred orientation to a varying extent was observed for all the oxides identified in the fired opaque porcelain. Similar results were observed on the XRD patterns for the fired opaque porcelain powder specimens (Fig. 1), except for an increased background between diffraction angles of 25° and 45°.

Prominent gold solid solution peaks were observed for all of the porcelain-fired specimens (Figs 2–5). This indicates that the incident X-ray beam penetrated through the ceramic layer and the metal-ceramic interface to reach the underlying alloy substrate.

For the Orion-ceramic specimen, where porcelain was fired on the oxidized surface (Fig. 2), In_2O_3, β-Ga_2O_3 leucite ($KAlSi_2O_6$), TiO_2, ZrO_2 and SnO_2 were identified. Excellent matches between the peaks observed and the ICDD powder diffraction files were found, with d-spacing differences generally within 0.01 Å, except for the leucite 114 and 332 peaks whose d-spacings were about 0.02 Å smaller than those from the

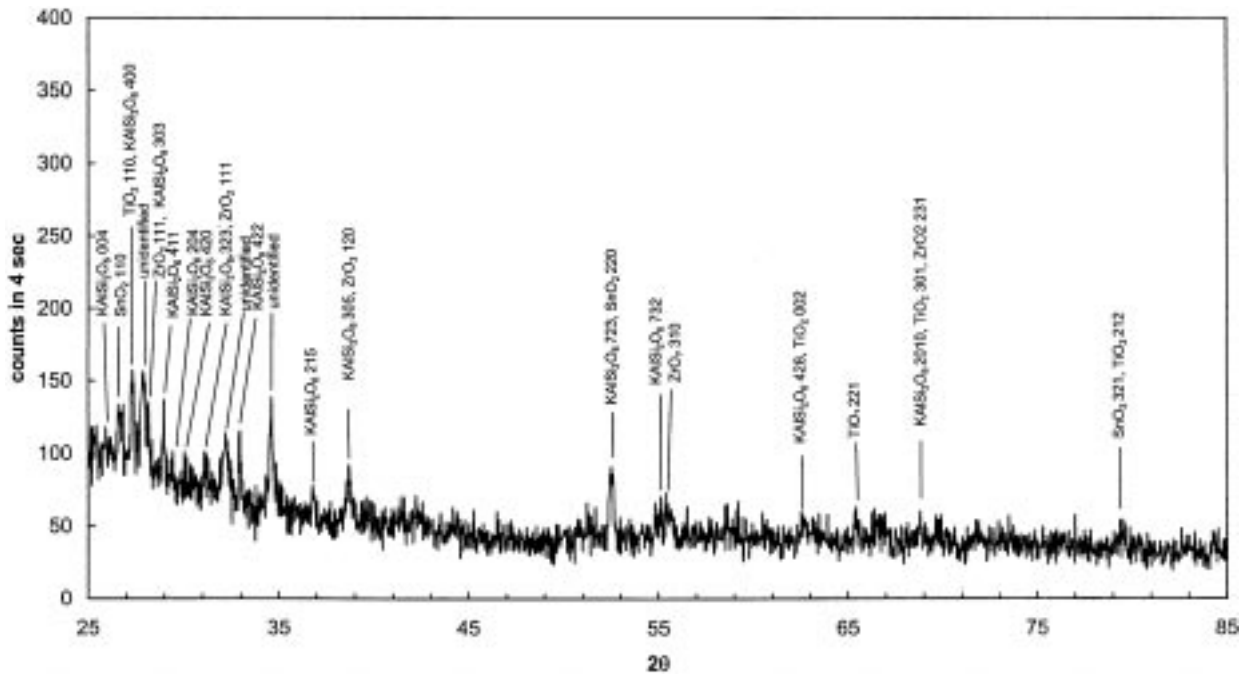

Figure 1 XRD pattern of fired Vita VMK opaque porcelain powder.

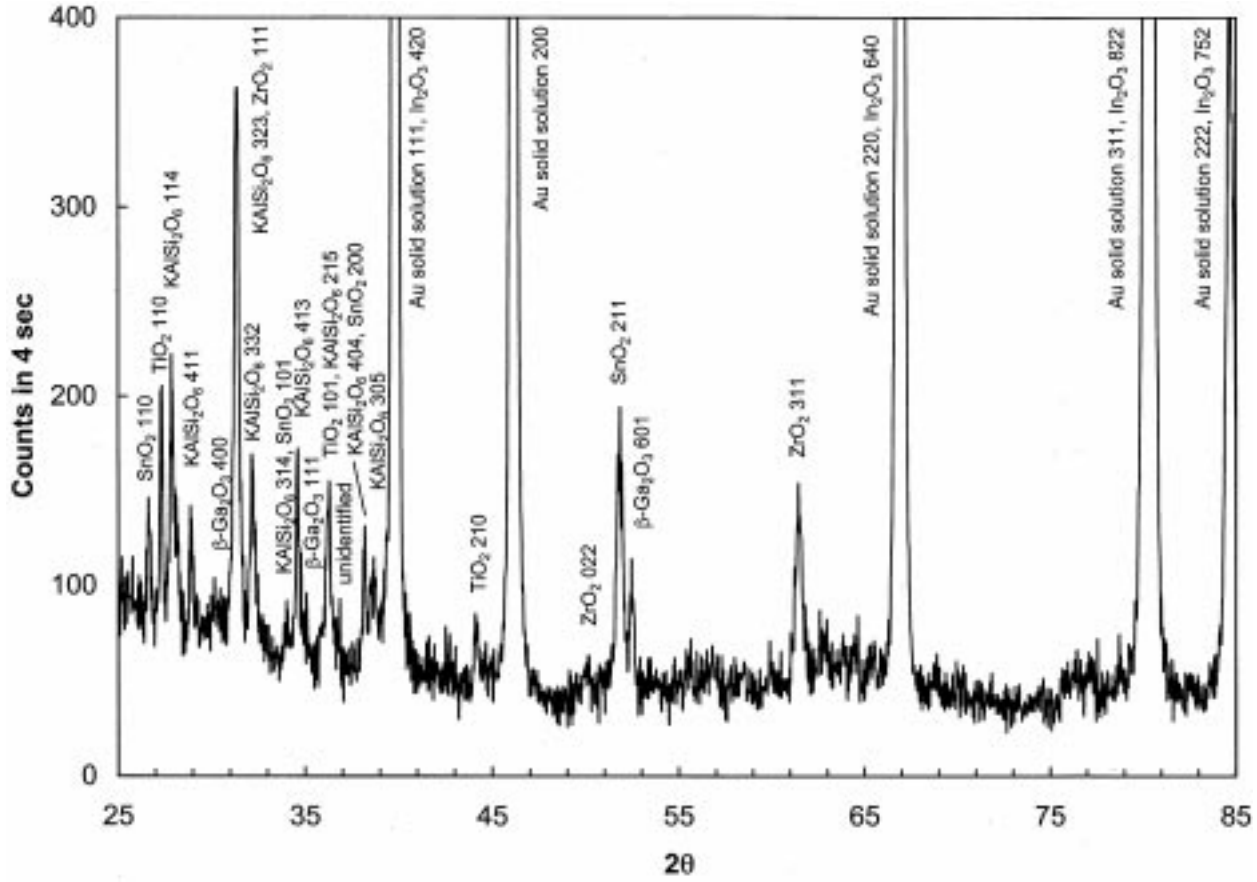

Figure 2 XRD pattern of Orion-ceramic (Vita VMK 68 opaque) interface. The alloy surface was oxidized before porcelain firing.

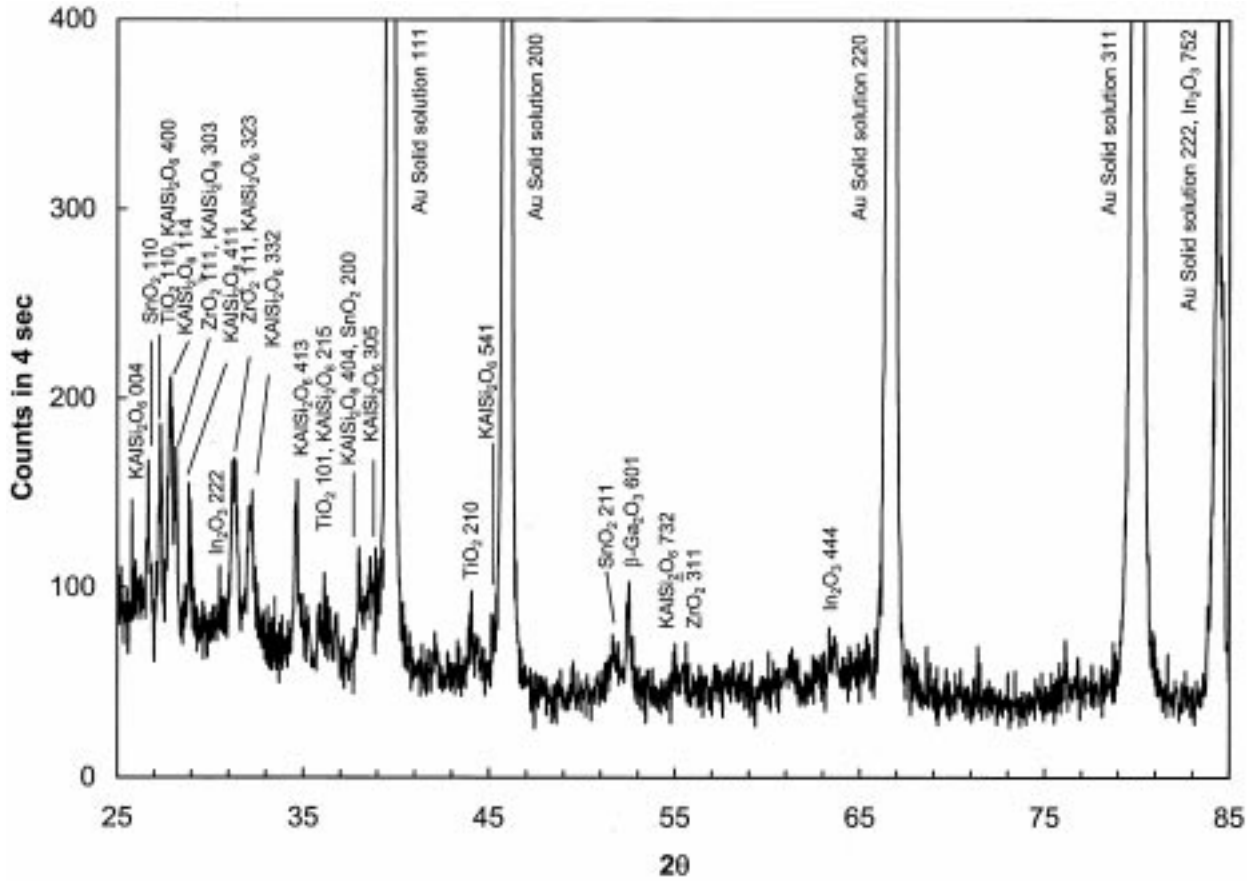

Figure 3 XRD pattern of Orion-ceramic (Vita VMK 68 opaque) interface. The alloy surface was not oxidized before porcelain firing.

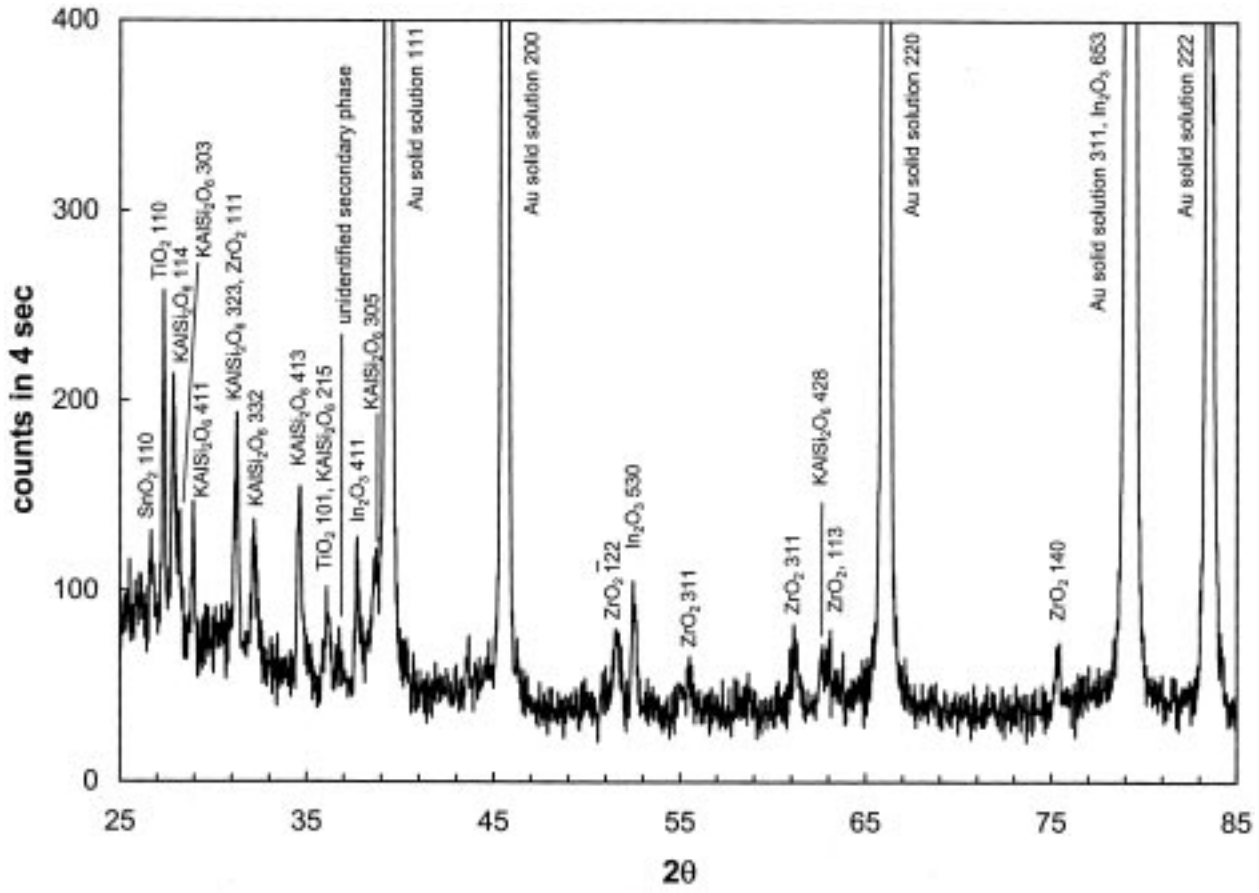

Figure 4 XRD pattern of Enaglaz I-ceramic (Vita VMK 68 opaque) interface. The alloy surface was oxidized before porcelain firing.

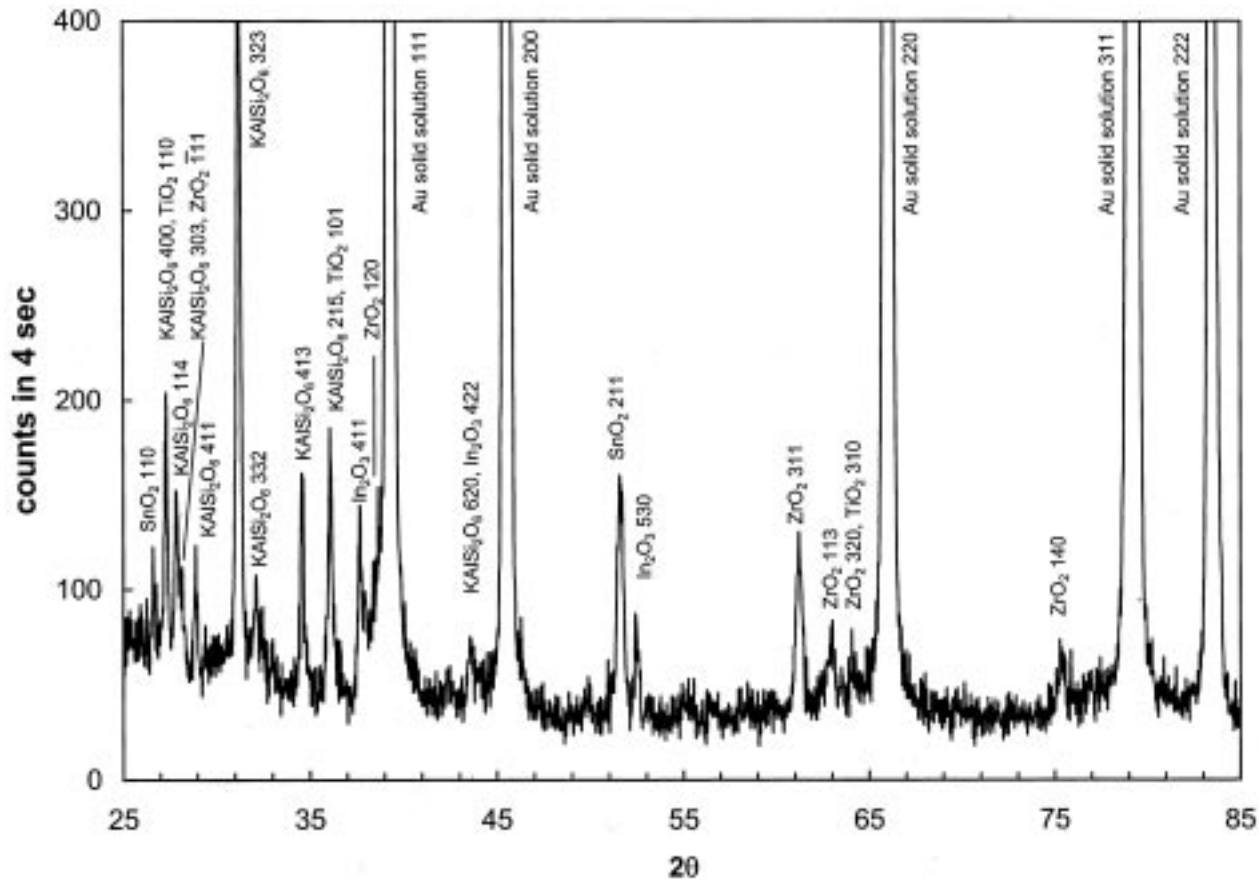

Figure 5 XRD pattern of Enaglaz I-ceramic (Vita VMK 68 opaque) interface. The alloy surface was not oxidized before porcelain firing.

file. A low-intensity peak with a d-spacing of 2.464 Å could not be matched to any of the oxides above and remains unidentified. Preferred crystallographic orientation was observed for the oxides identified at the alloy-ceramic interface.

For the Orion-ceramic specimen, where porcelain was fired on the alloy surface without pre-oxidation, In_2O_3, β-Ga_2O_3, leucite ($KAlSi_2O_6$), TiO_2, ZrO_2 and SnO_2 were identified (Fig. 3). Excellent matches between the peaks observed and the ICDD files were again found. Great similarity existed between the XRD patterns for the two Orion-ceramic specimens that differed in whether or not the alloy was oxidized before porcelain firing (Figs 2 and 3, respectively). When these two figures are compared, the intensity of the 211 peak for SnO_2 ($d = 1.76$ Å) in Fig. 3 appeared to be much lower than in Fig. 2. In addition, the 311 peak of ZrO_2 that was present on the XRD pattern when the alloy was oxidized, was absent when the alloy was not oxidized before porcelain firing. Preferred orientation was again observed for the oxides identified at the alloy-ceramic interface.

For the Enaglaz I-ceramic specimen where porcelain was fired on the oxidized alloy surface (Fig. 4), In_2O_3, SnO_2 leucite ($KAlSi_2O_6$), TiO_2, ZrO_2 were identified at the interface. Again, excellent matches between the peaks observed and the ICDD powder diffraction files were found, with d-spacing differences generally within 0.01 Å, except for the leucite 332 and 413 peaks whose d-spacings differed by about 0.02 Å from those on the ICDD file. A low-intensity peak with d-spacing of 2.444 Å can not be matched to any of the ICDD files, and was considered arisen from the unidentified secondary phase observed on the polished alloy specimens. Preferred crystallographic orientation was again also observed for the oxides identified at the alloy-ceramic interface.

Great similarity was also found when the XRD patterns were compared for the Enaglaz I-ceramic specimens where the alloy was oxidized or not oxidized before porcelain firing (Figs 4 and 5, respectively). In_2O_3, SnO_2 leucite ($KAlSi_2O_6$), TiO_2 and ZrO_2 were identified at the interface, and these oxides again showed preferred orientation.

Lattice parameters for the face-centered cubic gold solid solutions of both alloys were determined for the four surface conditions described above, using the Nelson-Riley analysis [41] and linear regression. Minimum lattice parameter changes ($\leq 1\%$) for gold solid solutions were observed for both alloys at the four different conditions (Table III). In all cases, the lattice parameter for the gold solid solution was less than the value (4.079 Å) for pure gold [41].

4. Discussion

Compared to the XRD results recently found for four as-cast high-palladium alloys [48], the two gold-based alloys in the present study only exhibited slight preferred crystallographic orientation in the polished condition. The oxides found on the as-cast alloy surface are not surprising, given the reactive nature of In, Ga and Sn with oxygen. These oxides may have formed during the in-air casting procedure when the alloy was melted with an oxygen-gas torch or subsequently after metallographic polishing and before XRD analysis. However, significant quantities of oxide were not detected by XRD on the surfaces of four metallographically polished and etched as-cast high-palladium alloys [48]. Such difference is considered due to the etching of the alloy, which may remove most of the surface oxides. Small amounts of secondary phases are expected to exist in the two gold-based alloys, because of their complex multi-component compositions (Table I).

The oxide layer formed on the alloy surface at high temperatures plays a critical role in metal-ceramic bonding. In the present study, the oxides identified on the oxidized alloy surfaces were expected, based on their compositions. The preferred crystallographic orientation exhibited by all oxides suggests that special epitaxial relationships exist with the alloy substrate. Preferred orientation was previously observed for the oxides on the surfaces of representative oxidized Pd-Cu-Ga and Pd-Ga alloys, and was considered to contribute to the minimization of the alloy-oxide interfacial free energy and the strong bonding between the alloys and ceramic [43].

The less than perfect match for the two In_2O_3 peaks on the oxidized Enaglaz I is probably due to the preferred orientation of the oxides formed on the alloy surface. A similar result was previously observed by Brantley *et al.* [43], where the In_2O_3 phase found on two Pd-Ga alloys, that had been metallographically polished and etched before oxidation, had extreme preferred orientation. In contrast when these two alloys were instead air-abraded before oxidation, following the usual dental laboratory procedure, the dominant surface oxide was β-Ga_2O_3 and not In_2O_3. Consequently, the surface roughness and state of residual stress for the alloy can have important

TABLE III Lattice parameters for the gold solid solution in the alloys determined by Nelson-Riley linear regression analysis [41]

	Polished*	Oxidized†	Porcelain fired without pre-oxidation‡	Porcelain fired with pre-oxidation‡
Orion	3.999	3.982	3.993	3.983
Enaglaz I	4.049	4.036	4.033	4.032

*The data are the means of two values obtained with the Rigaku and Philips diffractometers on two specimens. The differences between individual values were less than 0.01 Å.

†The data are the means of the two values obtained from a single specimen with the Rigaku diffractometer. The differences between individual values were less than 0.01 Å.

‡The data are the means of a single value obtained with the Philips diffractometer and three values obtained with the Rigaku diffractometer from one specimen. The differences between individual values were less than 0.01 Å.

consequences for the oxide species formed during oxidation or porcelain firing. This may also explain the *d*-spacing differences between the observed leucite 114 peak for the pre-oxidized Orion-ceramic specimens and the corresponding peak from the ICDD file.

The oxides identified in the fired opaque VMK 68 porcelain, ($KAlSi_2O_6$, SnO_2, ZrO_2 and TiO_2) are in consistent agreement with previously published results [28, 49]. However, SnO_2 was not detected in another XRD study [44], presumably due to the composition of the particular dental porcelain used in that investigation. Preferred orientation for the oxides found in the fired opaque porcelain was observed previously by Miyagawa [44]. Perhaps this result arises because the oxide filler particles in the porcelain are not single crystals but rather aggregates of crystals. The preferred orientation of the crystals in these aggregates would be a consequence of the manufacturing technique used to prepare the original filler particles. The high background at the lower 2θ region between 25 and 45° was attributed to the diffuse incoherent scattering from the powder specimens [41].

At the Orion-ceramic interfaces, In_2O_3 and β-Ga_2O_3 were considered to originate from the alloy surface oxide layer, while the remainder of the oxides were present in the fired opaque porcelain. No additional oxides formed at the interface as the result of interactions between the various oxides. Similarly, for the Enaglaz I-ceramic interfaces, In_2O_3 originated from the alloy surface oxide layer, and the remainder of the oxides were present in the fired opaque porcelain. SnO_2 is assumed to arise from both the oxidized alloy surface and the porcelain. The present XRD results are consistent with previously published studies on gold alloy-ceramic interfaces [44, 45]. These results strongly support the chemical bonding theory [15, 20] at the metal-ceramic interface and emphasize the critical contribution of chemical bonding to porcelain adherence.

An earlier study [49] of the metal-ceramic interface using scanning electron microscopy (SEM) and microprobe analysis suggested that the oxides formed on the alloy surface may partially diffuse into the porcelain. Such diffusion would be enhanced by increasing the porcelain firing time and was considered to contribute to the metal-ceramic bonding. However, these hypotheses cannot be verified in the present study, due to the limited porcelain thickness on the specimen and the inability of the XRD method to determine elemental concentration profiles.

It is well known that residual stress at the metal-ceramic interfaces, arising from mismatch of the thermal contraction coefficients between alloy and ceramic (below its T_g), has an important role for strong metal-ceramic bonding [15, 18, 23]. Due to the limited penetration of X-rays [41], the thickness of the porcelain fired on the alloy substrate in the present study was intentionally designed to be less than 50 μm thick. Such a very thin layer of porcelain, compared to the customary opaque porcelain thickness of 0.2–0.3 mm, may not be able to induce the amount of residual stress normally existing at the metal-ceramic interface. This may have a subtle effect on the lattice parameters of the alloy structures near the interface, and the preferred orientation for the oxides observed in the present study. Pilot experiments where the normal thickness of opaque porcelain was fired to the alloy substrate, and the porcelain subsequently polished to a thickness of about 50 μm appeared to yield the same phases identified by XRD. Subsequently, this more cumbersome procedure was replaced by the preparation of 50 μm–thick porcelain layers.

Internal oxidation has been observed in oxidized dental gold alloys containing In and Sn [50]. In_2O_3 and SnO_2 were identified on the oxidized alloy surface and were considered relevant to the porcelain boding. Internal oxidation occurs through the diffusion of oxygen into the alloy and reaction with oxidizable base metal elements; a precipitation of the base metal oxides occurs at an advancing reaction front [51]. It is expected that internal oxidation may occur in the two gold alloys selected for this study. However, the present XRD methods are not capable of detecting such internal oxidation. Further study of carefully polished and etched specimens, using SEM with X-ray energy-dispersive spectroscopic analysis (EDS) and X-ray photoelectron spectroscopy (XPS), is required to verify its occurrence.

One of the alloys, Enaglaz I, in the present study does not require oxidation firing before the application of porcelain as recommended by its manufacturer, while the other alloy requires oxidation. From the results of this study, however, the reason behind such difference is still unknown.

The difference in the lattice parameters of the gold solid solution for the alloys can be explained by their elemental composition. Since both platinum and palladium have smaller atomic radii than gold [41], substitutional solid solutions with smaller lattice parameters are expected for gold-platinum and gold-palladium alloys. Further, because the atomic radius for platinum is larger than that for palladium and the gold content in Enaglaz I is higher than that in Orion, the lattice parameter for the as-cast Enaglaz I alloy is expected to be larger than that of Orion and closer to gold.

5. Conclusion

X-ray diffraction was used to characterize dental alloy-ceramic interfaces. For the polished alloy specimens, β-Ga_2O_3 and In_2O_3 were identified on the Au-Pd-In alloy surfaces and SnO_2 was detected on the Au-Pt-Pd-In alloy surfaces, in addition to prominent gold solid solution peaks.

After high temperature oxidation, β-Ga_2O_3 and In_2O_3, were identified on the Au-Pd-In alloy surfaces, while In_2O_3 and SnO_2 were detected on the Au-Pt-Pd-In alloy surfaces. Preferred orientation was observed for all the oxides identified.

Prominent gold solid solution peaks were observed for all the porcelain-fired specimens. For both of the alloys, oxides from the alloy surface oxidation layers and fired opaque porcelain were identified at the alloy-ceramic interfaces with no addition oxides. No major differences were found between the XRD patterns of alloy-ceramic specimens where ceramic was fired on the alloy with or without prior alloy oxidation.

Minimum lattice parameter changes ($<1\%$) for the gold solid solution were observed for both alloys before

and after the high temperature oxidation and porcelain firing.

The results from the present XRD study support the chemical bonding theory for metal-ceramic adhesion. Future study on the alloy-ceramic interfaces using X-ray photoelectron spectroscopy (XPS) and analytical transmission electron microscopy (TEM) will be necessary to further elucidate the adhesion mechanisms.

Acknowledgment

The authors wish to acknowledge Tokuriki Honten for providing Enaglaz I alloy for this study. The authors would like to thank Mrs Jeanne Santa Cruz for her assistance in the preparation of the manuscript.

References

1. J. W. MCLEAN, in ''The Science and Art of Dental Ceramics, Vol. I, The Nature of Dental Ceramics and Their Clinical Use'' (Quintessence, Chicago, 1979) p. 55.
2. J. COORNAERT, P. ADRIAENS and J. DE BOEVER, *J. Prosthet. Dent.* **51** (1984) 338.
3. M. WEINSTEIN and A. B. WEINSTEIN, US Patent 3,052,982 (1962).
4. J. W. WEINSTEIN, S. KATZ and A. B. WEINSTEIN, US Patent 3,052,983 (1962).
5. J. W. MCLEAN, *Oper. Dent.* **16** (1991) 149.
6. S. D. CAMPBELL, *J. Prosthet. Dent.* **62** (1989) 476.
7. J. P. MOFFA, W. A. JENKINS, J. A. ELLISON and J. C. HAMILTON, *ibid.* **52** (1984) 491.
8. K. J. ANUSAVICE, *J. Am. Dent. Assoc.* **124** (1993) 72.
9. G. MUMFORD, *Dent. Clin. North. Am.* **9** (1965) 241.
10. E. J. RILEY, *ibid.* **21** (1977) 669.
11. K. J. ANUSAVICE, in ''Proceedings of The Third International Symposium on Titanium in Dentistry'', Leura, New South Wales, Australia, 1995, p. 137.
12. G. PETZOW, T. SUGA, G. ELSSNER and M. TURWITT, in ''Sintered Metal-Ceramic Composites'', edited by G. S. Upadhyaya (Elsevier Science Publishers, Amsterdam, 1984) p. 3.
13. J. M. HOWE, *Inter. Mater. Rev.* **38** (1993) 233.
14. D. JONES, *Annals New York Acad. Sci.* **523** (1988) 19.
15. R. L. BERTOLOTTI, in ''Dental Ceramics, The First International Symposium on Ceramics'', edited by J. W. McLean, Los Angeles, CA, 1983 (Quintessence, Los Angeles, CA, 1983) p. 414.
16. D. JONES, *Brit. Ceram. Transac. J.* **84** (1985) 40.
17. I. A. HAMMAD and Y. F. TALIC, *J. Prosthet. Dent.* **75** (1996) 602.
18. M. BAGBY, S. J. MARSHALL and G. W. MARSHALL Jr. *Ibid.* **63** (1990) 21.
19. J. A. PASK and R. M. FULRATH, *J. Am. Ceram. Soc.* **45** (1962) 592.
20. J. A. PASK, in ''Alternatives to Gold Alloys in Dentistry'' edited by T. M. Valega, Sr. (U.S. DHEW, Bethesda, MD, 1977) p. 235.
21. E. P. LAUTENSCHLAGER, E. H. GREENER and W. E. ELKINGTON, *J. Dent. Res.* **48** (1969) 1206.
22. K. J. ANUSAVICE, J. A. HORNER and C. W. FAIRHURST, *ibid.* **56** (1977) 1045.
23. P. J. CASCONE, in ''Dental Porcelain, the State of the Art, 1977'' edited by H. N. Yamada (Los Angeles, CA, 1977) p. 109.
24. W. WAGNER, K. ASGAR, W. BIGELOW and R. FLINN, *J. Biomed. Mater. Res.* **27** (1993) 531.
25. R. D. RINGLE, J. R. MACKERT, JR and C. W. FAIRHURST, *J. Dent. Res.* **62** (1983) 933.
26. J. MACKERT Jr, R. D. RINGLE, E. E. PARRY, A. L. EVENS and C. W. FAIRHURST, *ibid.* **67** (1988) 474.
27. Y. WU, J. B. MOSER, L. M. JAMESON and W. F. MALONE, *J. Prosthet. Dent.* **66** (1991) 439.
28. W. J. O'BRIEN and G. RYGE, *J. Am. Ceram. Soc.* **47** (1964) 5.
29. S. BROOKS, in ''Dental Porcelain, the State of the Art, 1977'' edited by H. N. Yamada (Los Angeles, CA, 1977) p. 157.
30. M. A. CARPENTER and R. J. GOODKIND, *J. Prosthet. Dent.* **42** (1979) 86.
31. J. M. CARTER, J. AL-MUDAFAR and S. E. SORENSEN, *ibid.* **41** (1979) 167.
32. ''Skinner's Science of Dental Material'', 8th edn, edited by R. W. Philips, (Saunders, Philadelphia, 1982) p. 521.
33. ''Restorative Dental Materials'', 10th edn, edited by R. G. CRAIG (Mosby, St. Louis, 1996) p. 486.
34. J. J. TUCCILLO and P. J. CASCONE, in ''First International Symposium on Ceramics'', Los Angeles, CA, 1983, edited by J. W. McLean, (Quintessence, Los Angeles, CA, 1983) p. 347.
35. S. TWIGGS, D. HASHINGER, R. MORENA and C. FAIRHURST, *J. Biomed. Mater. Res.* **20** (1986) 293.
36. S. W. TWIGGS, J. R. SEARLE, R. D. RINGLE and C. W. FAIRHURST, *J. Dent. Res.* **68** (1989) 1316.
37. C. W. FAIRHURST, D. T. HASHINGER and S. W. TWIGGS, *ibid.* **68** (1989) 1313.
38. J. MACKERT Jr and A. EVANS, *ibid.* **70** (1991) 137.
39. T. WALTON and W. O'BRIEN, *ibid.* **64** (1985) 476.
40. W. J. O'BRIEN, in ''Dental Porcelain, the State of the Art, 1977'', edited by H. N. Yamada, (Los Angeles, CA, 1977) p. 137.
41. B. D. CULLITY, in ''Elements of X-Ray Diffraction'', 2nd. edn (Addison-Wesley, Reading, MA, 1978), pp. 107, 179, 292, 356.
42. H. OHNO, Y. KANZAWA and Y. YAMANE, *Dent. Mater. J.* **2** (1983) 59.
43. W. A. BRANTLEY, Z. CAI, E. PAPAZOGLOU, J. C. MITCHELL, S. J. KERBER, G. P. MANN and T. L. BARR, *Dent. Mater.* **12** (1996) 333.
44. Y. MIYAGAWA, *Jpn. J. Dent. Mater.* **18** (1977) 296.
45. *Iden., ibid.* **19** (1977) 15.
46. M. BAGBY, S. MARSHALL and G. MARSHALL, *J. Appl. Biomater.* **1** (1990) 31.
47. J. R. MACKERT JR, T. G. CONNER, R. D. RINGLE, E. E. PARRY and C. W. FAIRHURST, *J. Am. Ceram. Soc.* **75** (1992) 3087.
48. W. A. BRANTLEY, Z. CAI, D. W. FOREMEN, E. PAPAZOGLOU and J. C. MITCHELL, *Dent. Mater.* **11** (1995) 154.
49. J. N. NALLY and J. M. MEYER, *Schweiz Monatsschr Zahnheilk* **80** (1970) 250.
50. H. OHNO, Y. KANZAWA, I. KAWASHIMA and N. SHIOKAWA, *J. Dent. Res.* **62** (1983) 774.
51. J.L. MEIJERING, in ''Advances in Materials Research'', edited by H. Hermann (John Wiley & Sons, New York, 1971) p. 1.

Received 7 September 1999
and accepted 26 January 2000